

基于原位配体反应的锰(II)配位聚合物的合成、结构和催化性质

赵素琴^{*1} 顾金忠^{*2}

(¹青海民族大学物理与电子信息工程学院, 西宁 810007)

(²兰州大学化学化工学院, 兰州 730000)

摘要: 采用水热方法, 选用含2个氰基的醚氧桥联羧酸配体(Hdbna)和2,2'-联吡啶(2,2'-bipy)与MnCl₂·4H₂O反应, 合成了一个二维配位聚合物[Mn(μ₃-Hdpna)(2,2'-bipy)]_n (**1**), 并对其结构和催化性质进行了研究。在配合物**1**中, 配体Hdbna在水热反应条件下, 通过原位反应被转化成醚氧桥联三羧酸配体(H₃dpna)。结构分析结果表明配合物**1**的晶体属于三斜晶系, $P\bar{1}$ 空间群。配合物**1**具有二维层结构。研究表明, 配合物**1**在硅腈化反应中表现出较高的催化活性。

关键词: 配位聚合物; 醚氧桥联三羧酸; 催化性质; 原位反应

中图分类号: O614.71⁺1 文献标识码: A 文章编号: 1001-4861(2021)04-0751-07

DOI: 10.11862/CJIC.2021.080

Synthesis, Structure and Catalytic Properties of Mn(II) Coordination Polymer through *in Situ* Ligand Reaction

ZHAO Su-Qin^{*1} GU Jin-Zhong^{*2}

(¹College of Physics and Electronic Information Engineering, Qinghai University for Nationalities, Xining 810007, China)

(²College of Chemistry and Chemical Engineering, Lanzhou University, Lanzhou 730000, China)

Abstract: One 2D coordination polymer, namely [Mn(μ₃-Hdpna)(2,2'-bipy)]_n (**1**), has been constructed hydrothermally using Hdbna (Hdbna=5-(2,3-dicyanobenzyloxy)nicotic acid), 2,2'-bipy (2,2'-bipy=2,2'-bipyridine), and manganese chloride at 160 °C. Interestingly, the H₃dpna (H₃dpna=5-(2,3-dicarboxylphenoxy)nicotic acid) ligand was generated by *in situ* hydrolysis of cyano groups in Hdbna. The product was isolated as stable crystalline solid and was characterized by IR spectrum, elemental analysis, thermogravimetric analysis (TGA), and single-crystal X-ray diffraction analysis. Single-crystal X-ray diffraction analysis reveals that compound **1** crystallizes in the triclinic system, space group $P\bar{1}$. Compound **1** discloses a 2D sheet with an *hcb* topology. Compound **1** was applied as an efficient heterogeneous catalyst for the cyanosilylation. CCDC: 2025016.

Keywords: coordination polymer; ether-bridged tricarboxylic acid; catalytic properties; *in situ* reaction

0 Introduction

In recent years, the design and hydro(solvo)thermal *in situ* syntheses of metal-organic coordination polymers have attracted great interest in the field of coordination chemistry and organic chemistry not only

because of their intriguing architectures and topologies, but also for that they have shown a variety of potential applications in catalysis, magnetism, luminescence and gas absorption^[1-8]. Compared with the traditional synthesis method, hydrothermal and solvothermal method could create more chances for *in situ* syn-

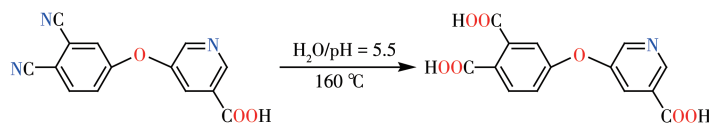
收稿日期: 2020-11-16。收修改稿日期: 2020-12-21。

青海省应用基础研究项目(No.2020-ZJ-705)资助。

*通信联系人。E-mail: qhzhqs@sina.com, gujzh@lzu.edu.cn

these of ligands due to the reaction conditions of high temperature and high pressure^[9-12]. At the same time, the hydro(solvo)thermal method has demonstrated increasing success in providing alternative pathways to crystalline complexes with *in situ* synthesized ligands which are difficult to obtain by routine synthetic methods.

Following our interest in the exploration of novel and poorly investigated multicarboxylic acids for the design of coordination polymers^[13-17], recently, we began to construct coordination polymers by use of the advantage of *in situ* ligand reaction. On the basis of current research on *in situ* ligand reaction, the carboxylate-



Scheme 1 H₃dpna ligand formed via *in situ* reaction

1 Experimental

1.1 Reagents and physical measurements

All chemicals and solvents were of AR grade and used without further purification. Carbon, hydrogen and nitrogen were determined using an Elementar Vario EL elemental analyzer. IR spectrum was recorded using KBr pellets and a Bruker EQUINOX 55 spectrometer. Thermogravimetric analysis (TGA) data were collected on a LINSEIS STA PT1600 thermal analyzer with a heating rate of 10 °C · min⁻¹. Powder X-ray diffraction (PXRD) patterns were measured on a Rigaku-Dmax 2400 diffractometer using Cu K α radiation (λ = 0.154 06 nm); the X-ray tube was operated at 40 kV and 40 mA. The data collection range was between 5° and 45°. Solution ¹H NMR spectra were recorded on a JNM ECS 400M spectrometer.

1.2 Synthesis of [Mn(μ_3 -Hdpna)(2,2'-bipy)]_n (**1**)

A mixture of MnCl₂ · 4H₂O (0.040 g, 0.2 mmol), Hdbna (0.053 g, 0.2 mmol), 2,2'-bipy (0.031 g, 0.2 mmol), NaOH (0.016 g, 0.4 mmol), and H₂O (10 mL) was stirred at room temperature for 15 min, and then sealed in a 25 mL Teflon-lined stainless steel vessel, and heated at 160 °C for 3 d, followed by cooling to room temperature at a rate of 10 °C · h⁻¹. Yellow block-

based ligands can be *in situ* generated from the CN-containing ligands precursor^[7,18-19]. Thus, the precursor we selected is 5-(2,3-dicyanobenoxy)nicotinic acid (Hdbna) due to its following characteristics: (1) it contains one carboxylate and two CN groups, which can form a tricarboxylate ligand through *in situ* ligand reaction (Scheme 1); (2) its corresponding acid, 5-(2,3-dicarboxylphenoxy)nicotinic acid (H₃dpna), still remain largely unexplored in the construction of coordination polymers^[20].

Herein, we report the synthesis, crystal structure, and catalytic properties of Mn(II) coordination polymer with H₃dpna ligands.

shaped crystals were isolated manually, and washed with distilled water. Yield: 55% (based on Hdbna). Anal. Calcd. for C₂₄H₁₅MnN₃O₇(%): C 56.26, H 2.95, N 8.20; Found(%): C 56.48, H 2.93, N 8.16. IR (KBr, cm⁻¹): 1 688w, 1 598m, 1 553s, 1 470s, 1 437s, 1 412m, 1 371m, 1 301w, 1 256m, 1 210w, 1 148w, 1 062w, 1 017w, 976w, 905w, 844w, 819w, 794w, 761m, 736w, 716w, 695w, 629w.

The compound is insoluble in water and common organic solvents, such as methanol, ethanol, acetone and DMF.

1.3 Structure determination

The single crystal with dimensions of 0.24 mm × 0.21 mm × 0.20 mm was collected at 293(2) K on a Bruker SMART APEX II CCD diffractometer with Cu K α radiation (λ = 0.154 178 nm). The structure was solved by direct methods and refined by full matrix least-square on F^2 using the SHELXTL-2014 program^[21]. All non-hydrogen atoms were refined anisotropically. All the hydrogen atoms were positioned geometrically and refined using a riding model. A summary of the crystallography data and structure refinement for **1** is given in Table 1. The selected bond lengths and angles for compound **1** are listed in Table 2. Hydrogen bond parameters of compound **1** are given in Table 3.

Table 1 Crystal data for compound 1

Formula	C ₂₄ H ₁₅ MnN ₃ O ₇	<i>F</i> (000)	522
Formula weight	512.33	θ range for data collection / (°)	3.606~65.998
Crystal system	Triclinic	Limiting indices	-9 ≤ <i>h</i> ≤ 7, -12 ≤ <i>k</i> ≤ 13, -15 ≤ <i>l</i> ≤ 15
Space group	<i>P</i> $\bar{1}$	Reflection collected, unique (<i>R</i> _{int})	6 931, 3 547 (0.076 5)
<i>a</i> / nm	0.784 98(8)	<i>D</i> _c / (g·cm ⁻³)	1.617
<i>b</i> / nm	1.130 30(13)	μ / mm ⁻¹	5.592
<i>c</i> / nm	1.290 01(11)	Data, restraint, parameter	3 547, 0, 317
α / (°)	73.119(9)	Goodness-of-fit on <i>F</i> ²	1.015
β / (°)	79.443(8)	Final <i>R</i> indices [<i>I</i> ≥ 2σ(<i>I</i>)] <i>R</i> ₁ , <i>wR</i> ₂	0.067 5, 0.149 9
γ / (°)	75.309(10)	<i>R</i> indices (all data) <i>R</i> ₁ , <i>wR</i> ₂	0.119 4, 0.199 3
<i>V</i> / nm ³	1.052 0(2)	Largest diff. peak and hole / (e ⁻ ·nm ⁻³)	512 and -888
<i>Z</i>	2		

Table 2 Selected bond distances (nm) and bond angles (°) for compound 1

Mn1—O1	0.219 4(4)	Mn1—O2	0.230 7(4)	Mn1—O6A	0.208 5(4)
Mn1—N1B	0.222 7(5)	Mn1—N2	0.225 9(5)	Mn1—N3	0.228 5(5)
O6A—Mn1—O1	106.66(18)	O6A—Mn1—N1B	100.3(2)	O1—Mn1—N1B	90.28(18)
O6A—Mn1—N2	90.0(2)	N2—Mn1—O1	158.02(19)	N1B—Mn1—N2	101.0(2)
N3—Mn1—O6A	161.3(2)	O1—Mn1—N3	91.28(18)	N1B—Mn1—N3	84.60(19)
N2—Mn1—N3	71.3(2)	O6A—Mn1—O2	93.6(2)	O1—Mn1—O2	58.29(16)
O2—Mn1—N1B	148.27(18)	O2—Mn1—N2	107.48(18)	O2—Mn1—N3	91.34(19)

Symmetry codes: A: *x*, *y*+1, *z*; B: *x*+1, *y*, *z*.

Table 3 Hydrogen bond parameters of compound 1

D—H···A	<i>d</i> (D—H) / nm	<i>d</i> (H···A) / nm	<i>d</i> (D···A) / nm	∠DHA / (°)
O4—H4···O7	0.082 0	0.159 6	0.240 9	170.89

CCDC: 2025016.

1.4 Catalytic cyanosilylation of aldehydes

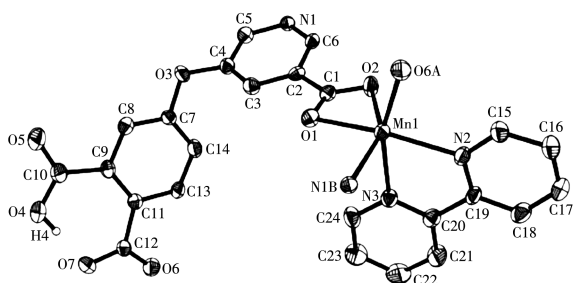
In a typical test, a suspension of an aromatic aldehyde (0.50 mmol, 4-nitrobenzaldehyde as a model substrate), trimethylsilyl cyanide (1.0 mmol) and catalyst (molar fraction: 3%) in dichloromethane (2.5 mL) was stirred at room temperature. After a desired reaction time, the catalyst was removed by centrifugation, followed by an evaporation of the solvent from the filtrate under reduced pressure to give a crude solid. This solid was dissolved in CDCl₃ and analyzed by ¹H NMR spectroscopy for quantification of products (Fig. S1, Supporting information). To perform the recycling experiment, the catalyst was isolated by centrifugation, washed with dichloromethane, dried at room temperature, and reused. The subsequent steps were performed as described above.

2 Results and discussion

2.1 Description of the structure

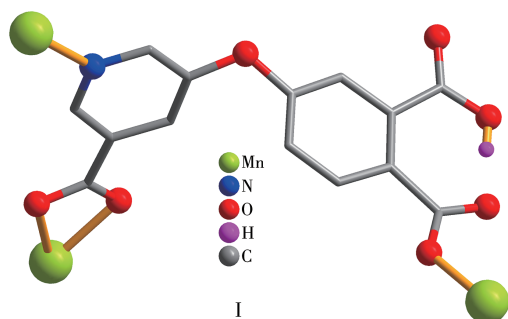
X-ray crystallography analysis reveals that compound **1** crystallizes in the triclinic system space group *P* $\bar{1}$. As shown in Fig. 1, the asymmetric unit of **1** bears one crystallographically unique Mn(II) atom, one μ_3 -Hdpna²⁻ block, and one 2,2'-bipy. The Mn1 center is six-coordinated and forms a distorted octahedral {MnN₃O₃} geometry. It is completed by three carboxylate O and one N atoms from three μ_3 -Hdpna²⁻ blocks and two N atoms from the 2,2'-bipy moiety. The Mn—O and Mn—N bond distances are 0.208 5(4)~0.230 7(4) nm and 0.222 7(5)~0.228 5(5) nm, respectively; these are within the normal ranges observed in related Mn(II) compounds^[15-17]. In **1**, the Hdpna²⁻ ligand adopts the coordination mode I (Scheme 2) with two deprotonat-

ed carboxylate groups being monodentate or bidentate. In the Hdpna^{2-} ligand, a dihedral angle (between two aromatic rings) and a $\text{C}-\text{O}_{\text{ether}}-\text{C}$ angle are 69.75° and 116.43° , respectively. The $\mu_3\text{-Hdpna}^{2-}$ ligands connect Mn1 atoms to give a 2D sheet (Fig.2). This sheet is composed of the 3-connected, topologically equivalent Mn1 and $\mu_3\text{-Hdpna}^{2-}$ nodes (Fig.3). The resulting net can be described as a uninodal 3-connected layer with an *hcb* (Shubnikov hexagonal plane net/(6,3)) topology

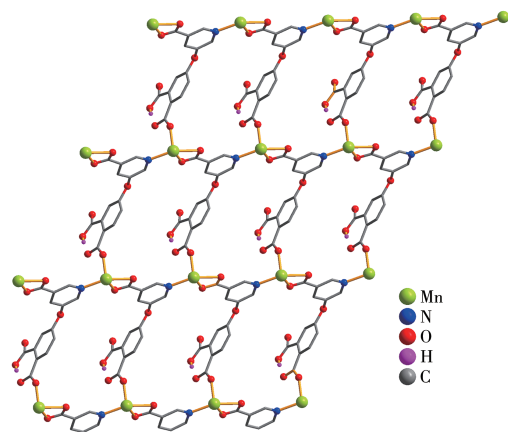


H atoms are omitted for clarity except those of COOH groups; Symmetry codes: A: $x, y+1, z$; B: $x+1, y, z$

Fig.1 Drawing of asymmetric unit of compound **1** with 30% probability thermal ellipsoids

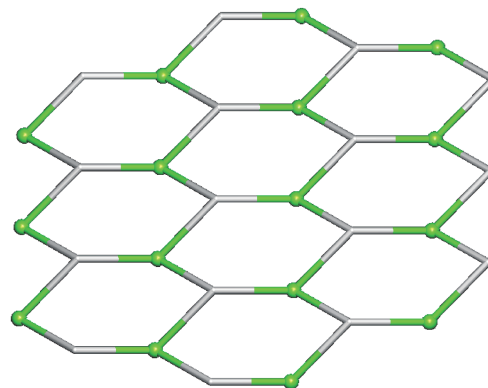


Scheme 2 Coordination mode of Hdpna^{2-} ligand in compound **1**



2,2'-bipy ligands are omitted for clarity

Fig.2 Perspective of 2D sheet along a and b axes in **1**



3-connected Mn1 nodes: green balls, centroids of 3-connected $\mu_3\text{-Hdpna}^{2-}$ nodes: gray

Fig.3 Topological representation of uninodal 3-connected metal-organic layer with *hcb* (Shubnikov hexagonal plane net/(6,3)) topology viewed along c axis

and point symbol of (6^3) .

2.2 TGA analysis

To determine the thermal stability of compound **1**, its thermal behavior was investigated under nitrogen atmosphere by TGA. As shown in Fig.4, compound **1** did not contain solvent of crystallization or H_2O ligands and remained stable up to 312°C , followed by a decomposition on further heating.

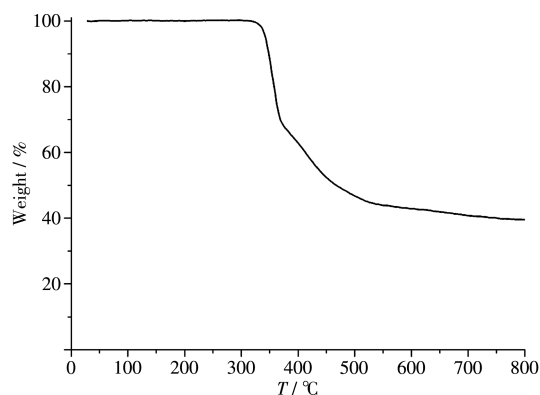


Fig.4 TGA curve of compound **1**

2.3 Catalytic cyanosilylation of aldehydes

Given the potential of manganese(II) coordination compounds to catalyze the organic reactions^[22-23], we explored the application of **1** as a heterogeneous catalyst in the cyanosilylation of 4-nitrobenzaldehyde as a model substrate to give 2-(4-nitrophenyl)-2-((trimethylsilyl)oxy)acetonitrile. Typical tests were carried out by reacting a mixture of 4-nitrobenzaldehyde, trimethylsilyl cyanide (TMSCN) and a Mn catalyst in dichloro-

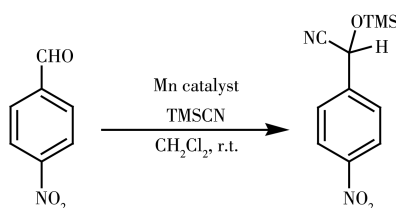
methane at room temperature (Scheme 3, Table 4). Such effects as reaction time, catalyst loading, solvent composition, catalyst recycling and finally substrate scope were investigated.

Upon using compound **1** as the catalyst (molar fraction: 3%), a high conversion of 82% of 4-nitrobenzaldehyde into 2-(4-nitrophenyl)-2-((trimethylsilyl)oxy) acetonitrile was reached after 12 h in dichloromethane at room temperature (Table 4, Entry 7). Upon extending the reaction time further to 18 h, only a slight increase in the product yield to 83% occurred. Moreover, no other products were detected, and the yield of this product was considered the conversion of 4-nitrobenzaldehyde (Fig.S1).

We also compared the activities of catalyst **1** in the reactions of other substituted aromatic and aliphatic aldehydes with trimethylsilyl cyanide, and the corresponding cyanohydrin derivatives were produced in

yields ranging from 43% to 82% (Table 5). Aryl aldehydes bearing strong electron-withdrawing substituents (*e.g.*, nitro and chloro) exhibited the higher reactivities (Table 5, Entry 2~5), which may be related to an increase in the electrophilicity of the substrate. Aldehydes containing electron-donating groups (*e.g.*, methyl) showed lower reaction yields (Table 5, Entry 7), as expected. An ortho-substituted aldehyde showed lower reactivity, possibly as a result of steric hindrance.

To examine the stability of **1** in the cyanosilylation reaction, we tested the recyclability of this heterogeneous catalyst. For this purpose, upon completion of a reaction cycle, we separated the catalyst by centrifugation, washed it with CH_2Cl_2 , and dried it at room temperature before its further use. The catalytic system maintained the high activity in at least five consecutive cycles (the yields were 80%, 80%, 79% and 78% for second to fifth run, respectively). According to the



Scheme 3 Mn-catalyzed cyanosilylation of 4-nitrobenzaldehyde (model substrate)

Table 4 Mn-catalyzed cyanosilylation of 4-nitrobenzaldehyde with TMSCN

Entry	Catalyst	Time / h	Catalyst loading / % (<i>n/n</i>)	Solvent	Yield* / %
1	1	1	3.0	CH_2Cl_2	29
2	1	2	3.0	CH_2Cl_2	53
3	1	4	3.0	CH_2Cl_2	62
4	1	6	3.0	CH_2Cl_2	69
5	1	8	3.0	CH_2Cl_2	75
6	1	10	3.0	CH_2Cl_2	78
7	1	12	3.0	CH_2Cl_2	82
8	1	12	2.0	CH_2Cl_2	63
9	1	12	4.0	CH_2Cl_2	84
10	1	12	3.0	CH_3CN	71
11	1	12	3.0	THF	63
12	1	12	3.0	CH_3OH	75
13	1	12	3.0	CH_3Cl	77
14	blank	12	—	CH_2Cl_2	3
15	MnCl_2	12	3.0	CH_2Cl_2	7
16	H_3dpna	12	3.0	CH_2Cl_2	6

* Calculated by ^1H NMR spectroscopy: $n_{\text{product}}/n_{\text{aldehyde}} \times 100\%$.

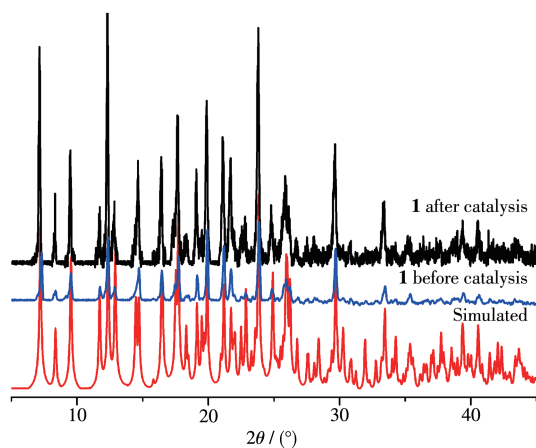
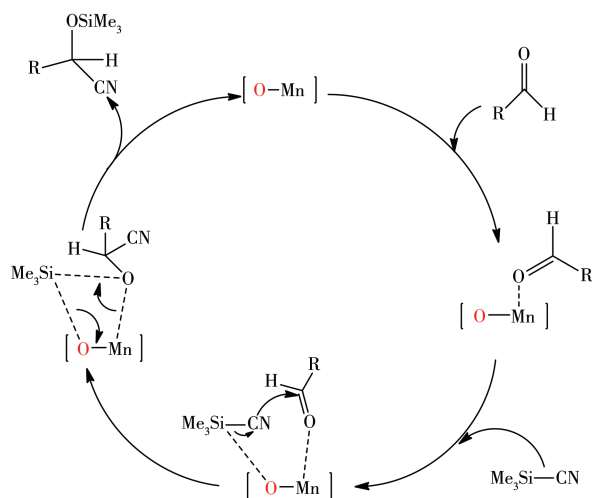
Table 5 Cyanosilylation of various aldehydes with TMSCN catalyzed by compound **1**^a

Entry	Substituted benzaldehyde substrate (R—C ₆ H ₄ CHO)	Product yield ^b / %
1	R=H	52
2	R=2-NO ₂	72
3	R=3-NO ₂	78
4	R=4-NO ₂	82
5	R=4-Cl	54
6	R=4-OH	48
7	R=4-CH ₃	43

^a Reaction condition: aldehyde (0.5 mmol), TMSCN (1.0 mmol), catalyst **1** (molar fraction: 3.0%) and CH₂Cl₂ (2.5 mL) at room temperature; ^b Calculated by ¹H NMR spectroscopy.

PXRD data (Fig. 5). the structure of **1** was essentially preserved after five catalytic cycles.

A possible catalytic cycle for the cyanosilylation reaction catalyzed by a Mn coordination polymer is proposed in Scheme 4. It can involve dual activation of the carbonyl and TMSCN by the Mn(II) centre and a ligated

Fig.5 PXRD patterns for **1**

Scheme 4 Mechanism for the Mn-catalyzed cyanosilylation reaction

carboxylate group, respectively, followed by the formation of the C—C bond leading to cyanohydrin^[24-25].

3 Conclusions

In summary, we have synthesized one Mn(II) coordination polymer **1** based on a tricarboxylate ligand generated by *in situ* reaction. Compound **1** shows a 2D sheet structure, and it exhibits a higher catalytic activity in the cyanosilylation at room temperature.

Supporting information is available at <http://www.wjhxhb.cn>

References:

- [1] Wang Q, Fan Y, Song, T Y, Xu J N, Wang J, Chai J, Liu Y L, Wang L, Zhang L R. *Inorg. Chim. Acta*, **2015**,**438**:128-134
- [2] Ding L, Zhong J C, Qiu X T, Sun Y Q, Chen Y P. *J. Solid State Chem.*, **2017**,**246**:138-144
- [3] Chen X M, Tong M L. *Acc. Chem. Res.*, **2007**,**40**(2):162-170
- [4] Wang C, Piel I, Glorius F. *J. Am. Chem. Soc.*, **2009**,**131**(12):4194-4195
- [5] Wu D, Bai X J, Tian H R, Yang W T, Li Z W, Huang Q, Du S Y, Sun Z M. *Inorg. Chem.*, **2015**,**54**(17):8617-8624
- [6] Rongere T, Langry A, Bennis K, Taviot-Gueho C, Ducki S, Leroux F. *J. Solid State Chem.*, **2018**,**268**:159-167
- [7] Li Y Y, Lu Y Q, Qiao X Y, Huang W M, Niu Y Y. *Inorg. Chem. Commun.*, **2020**,**118**:108002
- [8] Zhuang G M, Li X B, Gao E Q. *Inorg. Chem. Commun.*, **2014**,**47**:134-137
- [9] Wang X P, Zhao Y Q, Jagličić Z, Wang S N, Lin S J, Li X Y, Sun D. *Dalton Trans.*, **2015**,**44**(24):11013-11020
- [10] Chen Q H, Jiang F L, Chen L, Yang M, Hong M C. *Chem. Eur. J.*, **2012**,**18**(29):9117-9124
- [11] Dai F N, Cui P P, Ye F, Sun D F. *Cryst. Growth Des.*, **2010**,**10**(4):1474-1477
- [12] Sun D, Liu F J, Huang R B, Zheng L S. *Inorg. Chem.*, **2011**,**50**(24):12393-12395

- [13]Gu J Z, Wen M, Cai Y, Shi Z F, Nesterov D S, Kirillova M V, Kirillov A M. *Inorg. Chem.*, **2019**,**58**(9):5875-5885
- [14]邹训重, 吴疆, 顾金忠, 赵娜, 冯安生, 黎斌. 无机化学学报, **2019**, **35**(9):1705-1711
ZOU X Z, WU J, GU J Z, ZHAO N, FENG A S, LI Y. *Chinese J. Inorg. Chem.*, **2019**,**35**(9):1705-1711
- [15]Li Y, Wu J, Gu J Z, Qiu W D, Feng A S. *Chin. J. Struct. Chem.*, **2020**,**39**(4):727-736
- [16]Gu J Z, Cui Y H, Liang X X, Wu J, Lv D Y, Kirillov A M. *Cryst. Growth Des.*, **2016**,**16**(8):4658-4670
- [17]Gu J Z, Gao Z Q, Tang Y. *Cryst. Growth Des.*, **2012**,**12**(6):3312-3323
- [18]Hu T P, Bi W H, Hu X Q, Zhao X L, Sun D F. *Cryst. Growth Des.*, **2010**,**10**(8):3324-3326
- [19]Evans O R, Xiong R G, Wang Z Y, Wong G K, Lin W B. *Angew. Chem. Int. Ed.*, **1999**,**38**(4):536-538
- [20]Zhao Q, Luo B M, Fan H T, Feng Y Q, Liu X D, Deng Y L, Ma X. *Mater. Lett.*, **2017**,**197**:201-204
- [21]Spek A L. *Acta Crystallogr. Sect. C*, **2015**,**71**(1):9-18
- [22]Pal S, Maiti S, Nayek H P. *Appl. Organometal Chem.*, **2018**,**32**:e4447
- [23]Loukopoulos E, Kostakis G E. *J. Coord. Chem.*, **2018**,**71**(3):371-410
- [24]Karmakar A, Hazra S, da Silva M F C G, Pombeiro A J L. *Dalton Trans.*, **2015**,**44**(1):268-280
- [25]Aguirre-Díaz L M, Iglesias M, Snejko N, Gutiérrez-Puebla E, Monge M Á. *CrystEngComm*, **2013**,**15**(45):9562-9571